 ©2008 Kvantovaya Elektronika and Turpion Ltd

PACS numbers: 42.55.Px; 42.60.Jf; 42.60.Lh
DOI: 10.1070/QE2008v038n10ABEH013901

Optimisation of waveguide parameters of laser InGaAs/AlGaAs/GaAs heterostructures for obtaining the maximum beam width in the resonator and the maximum output power

A.P. Bogatov, T.I. Gushchik, A.E. Drakin, A.P. Nekrasov, V.V. Popovichev

***Abstract*. The waveguide design of a laser heterostructure is optimised to expand the laser beam in the vertical direction at the output mirror of a laser diode (up to 1.5 μm at the half intensity for the zero mode). Experimental samples of such diodes operated in the cw transverse single-mode lasing regime up to the output power of 0.5 W. The radiation divergence was $11^\circ - 12^\circ$ and $4^\circ - 7^\circ$ in the vertical and horizontal directions, respectively.**

Keywords: *expanded waveguide, transverse single-mode high-power ridge lasers.*

1. Introduction

An increase in the width of an optical beam from a diode laser is one of the ways to increase its output power. This is caused, in particular, by a decrease in the optical load on the output mirror of the laser diode, whose critical value (called the threshold of catastrophic optical degradation) is at present one of the main factors limiting the laser radiation power. The beam width can be increased both in the plane of the heterostructure layers and in the perpendicular direction. In the first case, it is determined by the size of the electric contact and in the second, – by the optical waveguide design of the heterostructure formed at the stage of its growth. In this paper, we consider the increase in the laser beam width by using the second approach and assume below that the beam width means its size in the vertical (with respect to the plane of layers) direction.

Many practical applications (for example, coupling of radiation into a single-mode fibre) require the laser diode to operate at the fundamental mode with a stable radiation pattern. Therefore, the simplest method for increasing the beam width, which involves the use of a weak optical waveguide (with jumps of the refractive index at the 10^{-3} level), proves unacceptable due to the effect of the pump current on the refractive indices of active layers, which will play a significant role in this case and lead to the instability of the radiation spot and its radiation pattern. Thus, the only way to expand the beam is the use of rather strong waveguides with an increased (up to several micrometers) width. However, in this case the waveguide becomes multimode and special conditions are required to produce discrimination of the mode gain for high-order modes, which is necessary for the operation at high radiation powers (see, for example, [1–6]).

In this paper we consider the InGaAs/AlGaAs/GaAs quantum-well heterostructure used to fabricate lasers emitting in the region from 0.94 to 1.14 μm. The heterostructure optimised to expand the beam provided the high output power of transverse single-mode ridge lasers manufactured from the optimised structure by preserving the diffraction divergence of the laser beam. This semiconductor heterostructure was chosen as the most technologically developed one, but the employed methods and approaches can be also used to optimise heterostructures based on other solid solutions.

It is clear that the optical beam expansion inevitably reduces the optical confinement factor, which, in turn, results in the decrease in the mode gain due to limitation of the material amplification developed in the active layers at reasonable pump currents. However, it is impossible to allow the drop in the mode gain to the level comparable with the nonresonance optical losses in the heterostructure because this leads to a drastic degradation of laser parameters – the increase in the lasing threshold and (which is most important for high-power lasers) the decrease in the slope efficiency. Because of this reason, the optimisation criterion for the heterostructure waveguide consists in obtaining the maximum beam width without a very steep drop in the mode gain, not below the level at which the slope efficiency significantly decreases and the lasing threshold considerably increases.

2. Heterostructure optimisation

Calculations were performed within the framework of the methods developed in [7, 8] and realised as the WAVE software product, which allows one to find the intensity distribution in the near-field region of laser radiation (the

A.P. Bogatov, T.I. Gushchik, A.E. Drakin P.N. Lebedev Physics Institute, Russian Academy of Sciences, Leninsky prosp. 53, 119991 Moscow, Russia; e-mail: GushhikTaras@yandex.ru;
A.P. Nekrasov, V.V. Popovichev Federal State Unitary Enterprise 'M.F. Stel'makh Polyus Research and Development Institute', ul. Vvedenskogo 3, 117342 Moscow, Russia

Received 28 May 2008
Kvantovaya Elektronika **38** (10) 935–939 (2008)
Translated by I.A. Ulitkin

Table 1. Layers of the basic nanoheterostructure.

Layer No.	Layer type	Layer composition	Layer thickness;
1	Metal contact	Au, Zn	–
2	Semiconductor contact layer	GaAs	d_2
3	p-emitter layer	$Al_xGa_{1-x}As$	d_3
4	Waveguide layer	$Al_yGa_{1-y}As$	d_4
5	Transition layer	GaAs	d_5
6	QW	$In_zGa_{1-z}As$	8 nm
7	Barrier layer	GaAs	d_7
8	QW	$In_zGa_{1-z}As$	8 nm
9	Transition layer	GaAs	d_9
10	Waveguide layer	$Al_vGa_{1-v}As$	d_{10}
11	n-emitter layer	$Al_wGa_{1-w}As$	d_{11}
12	Substrate	GaAs	–

intensity distribution at the output mirror) and in the far-field region.

Table 1 presents the composition of layers and their type in a basic nanoheterostructure in the most general form. The thickness of active QWs was set equal to 8 nm and the composition corresponded to lasing at 980 nm. Optimisation was performed by selecting the values x, y, v, w and thicknesses of passive layers characterising the heterostructure parameters.

The nanoheterostructure was modified by using the following general considerations. The field amplitude $u_j(x)$ in the jth layer has the form

$$u_j(x) = A_j \exp(iq_j x) + B_j \exp(-iq_j x), \tag{1}$$

where $q_j = (\omega^2 \varepsilon_j / c^2 - \beta^2)^{1/2}$; A_j, B_j, and β are found by solving the wave equation with the corresponding boundary conditions; x is the transverse coordinate; ε_j is the complex value of the permittivity of the jth layer; β is the complex propagation constant along the z axis.

It follows from (1) that the change rate of the field amplitude over the beam cross section in the j layer depends on q_j. To increase the beam width by increasing the thickness d_j of the selected layer, d_j should be close to the width to which we want the beam to be expanded. In addition, in this layer $u_j(x)$ should be a rather slow function, which requires the fulfilment of the inequality:

$$|q_j d_j| \leqslant 1, \tag{2}$$

in this case, the imaginary part in ε_j should be rather small because the layer in which the main part of the optical flux propagates cannot have large losses. Otherwise, the laser will have low radiative characteristics and be of no practical interest. Taking this into account, condition (2) can be rewritten in the form

$$\Delta n = |n_j - n_{\text{eff}}| \leqslant \lambda^2 / (8\pi^2 d_j^2 n_j), \tag{3}$$

where n_j is the refractive index of the jth layer; λ is the wavelength in vacuum; n_{eff} is the effective refractive index for the wave which corresponds to the waveguide eigenmode having the propagation constant β, i.e.

$$n_{\text{eff}} = |\text{Re}\,\beta| \frac{\lambda}{2\pi}. \tag{4}$$

Thus, the condition for the beam expansion is the presence of a rather thick passive (waveguide) layer with low optical losses and with the refractive index close to the effective refractive index of the entire structure waveguide. The estimate of the right-hand side part of inequality (3) for $\lambda = 0.98$ μm, $d_j = 4$ μm and $n_j \simeq 3.4$ yields $\sim 2.2 \times 10^{-4}$. This value restricts the maximum of the difference between the refractive index of the jth layer and n_{eff} and, in this case, is small compared to the change in the refractive index (1×10^{-4}), which possibly appears due to a number of uncontrolled or poorly controlled mechanisms. They involve temperature gradients accompanying the laser operation, volume mechanical stresses produced during mounting the laser chip, initial optical inhomogeneities caused by the imperfection of the structure growth technology, and etc. All this means that the increase in the thickness d_j above 4 μm is hardly reasonable.

Table 2 presents the parameters of the optimised structure satisfying these requirements. Layer no. 10 (we will call it the expanding layer) of thickness $d_{10} = 4$ μm was selected as a layer in which the main part of the expanded beam propagates. The calculated near- and far-field radiation intensities are presented in Fig. 1. Figure 1a also shows the refractive index profile of the optimal structure. The values of the refractive index at 980 nm and the corresponding composition of the AlGaAs and GaAs solid solutions were interpolated from data in [9], for gold and InGaAs they were borrowed from [10] and [11], respectively, the refractive index of active layers being decreased compared to [11] to take into account the effect of injected carriers.

For the field amplitude not to change too fast in our expanding layer, the value n_{eff} should be close to the refractive index of this layer with an accuracy of 10^{-4}. Calculations showed that the change in n_{10} by varying v (the content of Al in the $Al_vGa_{1-v}As$ solution) in the range from 0.208 to 0.213 satisfies this requirement.

The obtained half-width of the optical beam (about 1.5 μm) is approximately three times larger than the beam half-width for typical heterostructures used at present. This is a significant result, because it allows the increase in the laser output power by three times as well. In this case, the beam divergence at the 0.5 level decreased down to $\sim 12^\circ$, while in a typical structure it is, as a rule, $\sim 30^\circ$. This is also

Table 2. Parameters of the optimised nanoheterostructure.

Layer No.	Layer type	Layer composition	Layer thickness/μm	Refractive index
1	Metal contact	Au	–	0.24
2	Semiconductor contact layer	GaAs	0.14	3.520
3	p-emitter layer	$Al_{0.3}Ga_{0.7}As$	0.9	3.362
4	Waveguide layer	$Al_{0.3}Ga_{0.7}As$	0.9	3.362
5	Transition layer	GaAs	0.036	3.528
6	QW	InGaAs	0.008	3.58
7	Barrier layer	GaAs	0.012	3.528
8	QW	InGaAs	0.008	3.58
9	Transition layer	GaAs	0.036	3.528
10	Waveguide layer	$Al_{0.21}Ga_{0.79}As$	4.00	3.412
11	n-emitter layer	$Al_{0.3}Ga_{0.7}As$	1.0	3.362
12	Substrate	GaAs	–	3.528

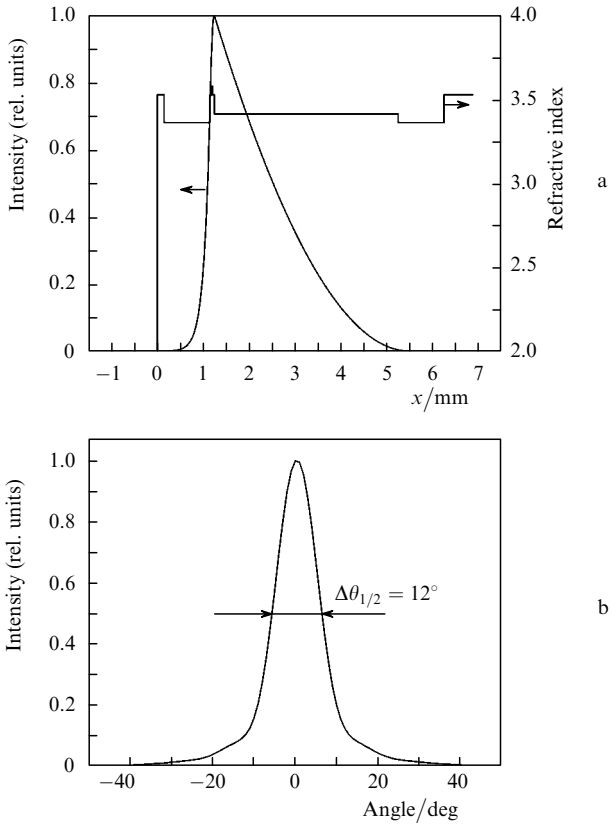

Figure 1. Calculated radiation intensity distributions at the output mirror (a) and far-field region (b) for the heterostructure from Table 2 in the direction perpendicular to the layers; Fig. 1a also shows the corresponding refractive index profile.

an important result because it significantly simplifies the solution of the problem of the optical matching of diode laser radiation with external optical systems, including optical beam collimators.

However, as stated above, the increase in the beam width is inevitably accompanied by the drop in the optical confinement factor and, as a result, by the decrease in the mode gain (approximately by six times compared to the standard structure). In our case, the optimal (trade-off) value of the optical confinement factor per active layer was $\sim 4.6 \times 10^{-3}$, which corresponded to the mode gain ~ 7.6 cm^{-1} for the material amplification in the quantum well 1000 cm^{-1} and for the nonresonance optical losses $\alpha = 2$ cm^{-1}.

It is well known that the slope efficiency of the laser action satisfies the relation

$$\eta \leqslant \alpha_m/(\alpha_m + \alpha), \tag{5}$$

where $\alpha_m = -\ln(R_1 R_2)/(2L)$ are mirror losses; R_1, R_2 are mirror reflectivities; L is the laser diode length. If we assume that the mirror reflectivities and the diode length are such that $\alpha_m = 7.6$ cm^{-1}, i.e. the mode gain obtained in calculations corresponds to the lasing threshold, then η will be no more than 79 %. The attempts to further increase the beam will result in the necessity to decrease α_m, which according to (5) definitely causes a decrease in η. It means that the key parameter in our problem is the nonresonance losses α. By decreasing them, we can decrease α_m while preserving η, for example, by increasing the resonator length. Therefore, in this case, a further decrease in the optical confinement factor as well as an increase in the optical beam width is possible.

3. Experiment

The samples fabricated based on the structures with parameters close to the optimised ones (see Table 2) were experimentally studied. Figure 2 shows a typical light–current characteristic of a ridge laser with the ridge parameters (the width 4 μm), which coincide with those used in paper [8]. For the currents from the threshold value (~80 mA) to ~400 mA, the light–current characteristic is close to the linear one with the slope efficiency ~62 % (0.8 A W^{-1}). As the current is further increased, the light–current characteristic becomes significantly sublinear. Nevertheless, for the current ~1000 mA, the laser output power achieves ~500 mW in the cw regime at room temperature of the sink. The difference of the obtained slope efficiency from its estimated quantity ($\leqslant 79$ %) is caused by the fact that according to (5) it depends on nonresonsnce losses α and mirror reflectifities R_1, R_2. Real values of these parameters can certainly differ from those used by us in the estimates.

The full-scale tests, which were performed under normal climatic conditions in the constant current operation regime corresponding to the 350-mW lasing power, showed that no decrease in the laser power was observed during 1000 hours of operation. Figure 3 presents the resource characteristic of one of the experimental samples.

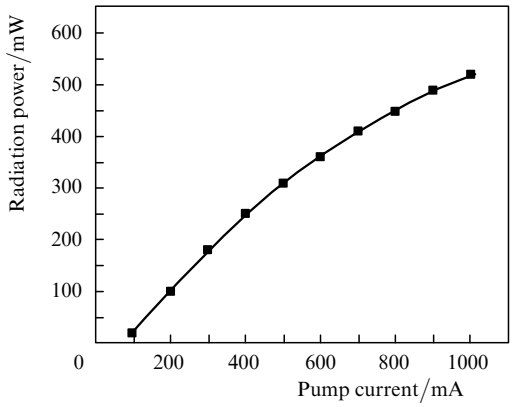

Figure 2. Typical experimental light–current characteristic of the cw transverse single-mode laser with an expanded waveguide at the room temperature of the sink.

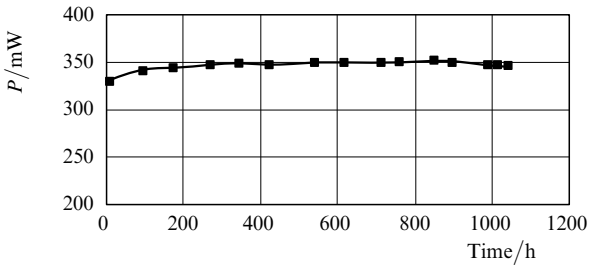

Figure 3. Typical resource characteristic of the transverse single-mode lasers under study at the constant pump current (551 mA) and temperature 28.5 °C.

The far-field intensity distribution for optimised lasers is presented in Fig. 4. The pump current is the parameter of the curves. One can see that the experimental results are close to calculated values [curve (4)]. Because for the optics of a diode laser the far-field intensity distribution is rather well correlated with the near-field intensity distribution, we can assume that the near-field intensity distribution is close to the calculated one.

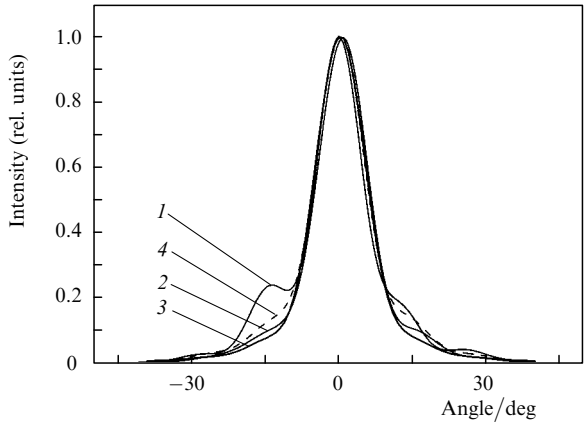

Figure 4. Far-field intensity distribution in the plane perpendicular to the heterolaser layers in the cw lasing regime at room temperature of the sink for pump currents 1 A (*1*), 800 (*2*) and 400 mA (*3*) and the calculated distribution (*4*).

Consider the discrepancy observed in Fig. 4 between calculated and experimental curves, which is present in the form of 'wings' in the far-field intensity distribution. In this case, the higher the current, the larger the wings, and therefore, their appearance is obviously the result of the thermal effect. This is confirmed by a noticeable sublinear increase in the power with the current exceeding ~400 mA. The temperature increase leads to changes in the refractive index of passive layers, in addition, the refractive index of active layers changes due to the increase in the electron concentration. Because the largest change in the refractive indices takes place near the active layers, then according to the property of the Fourier transform, the greatest effect from this change can be expected at the wings of the far-field intensity distribution. The temperature nature of the appearance of the wings in the cw far-field radiation distribution in the vertical direction was confirmed by the measurements performed in the pulsed regime (100 ns, 10 kHz). In the pulsed regime the stationary heating and temperature gradients do not appear and, hence, the radiation pattern in the entire range of pump currents remains almost constant and the wings in the far-field region are not observed (Fig. 5). The far-field distributions coincide in both regimes till the pump powers 400 mA.

Figure 6 shows the far-field radiation patterns in the horizontal plane in the cw operation regime. As the pump current is increased, the intensity distribution maximum shifted by ~0.8° due to the asymmetry of the imaginary part of the permittivity (absorption and amplification), which is obviously caused by the technological peculiarities of the ridge fabrication. In addition, the radiation pattern broadened (from 4.4° to 6.8° at half-maximum) due to the heating of the region below the ridge and some amplification of the horizontal waveguide caused by this heating. Nevertheless,

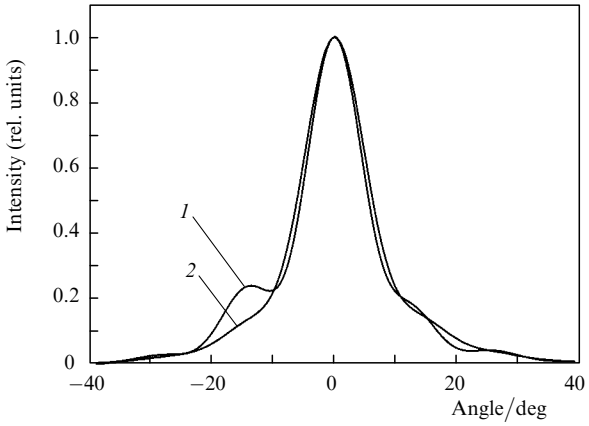

Figure 5. Far-field intensity distribution in the plane perpendicular to the heterolaser layers in the cw (*1*) and pulsed (*2*) regimes; the pump current is 1 A, the current pulse parameters: the duration is 100 ns, the pulse repetition rate is 10 kHz.

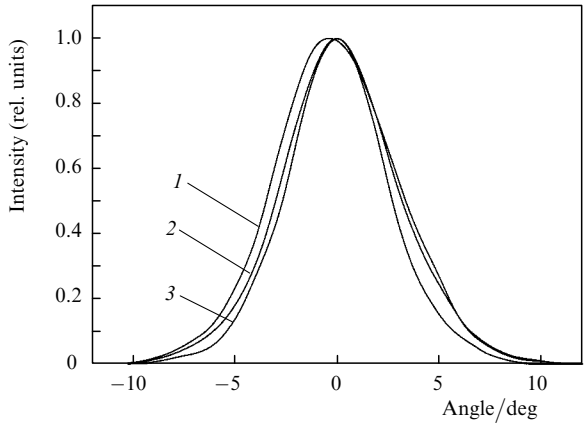

Figure 6. Far-field intensity distribution in the plane of the heterolaser layers in the cw lasing regime at room temperature of the sink for pump currents 1 A (*1*), 800 (*2*) and 400 mA (*3*).

in the entire range of pump currents, emission was transverse single-mode one.

Thus, we can state that according to the calculation results the laser heterostructure was optimised, which allowed the optical beam in the resonator to be significantly expanded while preserving its rather high radiative characteristics. Although the obtained results are based on the optimisation of the heterostructure with layers of the constant composition, nevertheless they can have a more general character. For example, if a heterostructure with a gradient distribution of the composition in the expanding layer is used for optimisation, it is easy to show in this case that the condition for the admissible variations in the refractive index in this layer will virtually coincide with condition (3). The difference will consist in the numerical factor of the order as that in (3). This can be easily confirmed if the Airy function is used instead of the exponentials in the right-hand side of Eqn (1).

Note also the peculiarity of this method of the beam expansion, which consists in a significant waveguide asymmetry. In the used waveguide the active region is located not in the middle but at the edge of the expanding layer. Calculations show that for the selected laser transverse mode this waveguide design provides the highest amplification selectivity with respect to other transverse modes.

4. Conclusions

Thus, it has been shown in this paper that by using the method of the waveguide engineering the optical beam width in the heterolaser resonator can be increased by several times (approximately by three times) compared to the similar value for typical heterolasers employed at present. In this case, the beam divergence in the vertical direction decreases to $11^\circ - 12^\circ$. The calculation results have been confirmed in the experiment. The output power of ~ 500 mW in the transverse single-mode lasing regime has been obtained. This creates the necessary prerequisites for fabricating more powerful, than at present, transverse single-mode heterolasers with increased beam brightness.

Acknowledgements. This work was partially supported by the programs 'Quantum nanostructures' of the Presidium of the RAS and 'Coherent optical radiation of semiconductor compounds and structures' of the Physical Sciences Division of the RAS as well as by the Federal Target Program 'Investigations and development in priority directions of the elaboration of the scientific and technological complex of Russia in 2007 – 2012' (State Contract No. 02.513.11.3168).

References

1. Buda M., van de Roer T.G., Kaufmann L.M.F., Iordache Gh., Cengher D., Diaconescu D., Petrescu-Prahova I.B., Haverkort Jos E.M., van der Vleuten W., Wolter J.H. *IEEE J. Sel. Top. Quantum Electron*., **3**, 173 (1997).
2. Al-Muhanna A., Mawst L.J., Botez D., Garbuzov D.Z., Martinelli R.U., Connolly J.C. *Appl. Phys. Lett*., **73**, 1182 (1998).
3. Lee J.J., Mawst L.J., Botez D. *IEEE Photonic. Technol. Lett*., **14**, 1046 (2002).
4. Buda M., Tan H.H., Aggett M.F., Jagadish C. US Patent No. US 2004/0013147 A1 (2004).
5. Ghislotti G., Bravetti P., Bacchin G. US Patent No. US 2004/0190575 A1 (2004).
6. Bezotosnyi V.V., Vasil'eva V.V., Vinokurov D.A., Kapitonov V.A., Krokhin O.N., Leshko A.Yu., Lyutetskii A.V., Murashova A.V., Nalet T.A., Nikolaev D.N., Pikhtin N.A., Popov Yu.M., Slipchenko S.O., Stankevich A.L., Fetisova N.V., Shamakhov V.V., Tarasov I.S. *Fiz. Tekhn. Poluprovodn*., **42**, 357 (2008).
7. Stratonnikov A.A., Bogatov A.P., Drakin A.E., Kamenets F.F. *J. Opt. A: Pure Appl. Opt*., **4**, 535 (2002).
8. Popovichev V.V., Davydova E.I., Marmalyuk A.A., Simakov A.V., Uspenskii M.B., Chel'nyi A.A., Bogatov A.P., Drakin A.E., Plisyuk S.A., Stratonnikov A.A. *Kvantovaya Elektron*., **32**, 1099 (2002) [*Quantum Electron*., **32**, 1099 (2002)].
9. Adachi S. (Ed.) *Properties of Aluminum Gallium Arsenide* (London: INSPEC, IEE, 1993).
10. Palik E.D. (Ed.) *Handbook of optical constants of solid* (NY: Acad. Press, 1985) Part I.
11. Zou W.X., Merz J.L., Coldren L.A. *J. Appl. Phys*., **72**, 5047 (1992).